Intermittent and quasiperiodic behavior in a Zeeman laser model with large cavity anisotropy

Javier Redondo, Germán J. de Valcárcel, and Eugenio Roldán
Departament d'Òptica, Universitat de València, Dr. Moliner 50, 46100 Burjassot, Spain
(Received 3 March 1997; revised manuscript received 17 June 1997)

The stability and dynamic behavior of a two-level, $J=0\leftrightarrow J=1$, Zeeman laser model is investigated in the limit of large cavity anisotropy. The stability of the steady-state solutions is governed by two different Hopf bifurcations, one affecting the polarization state of the laser light and the other affecting the intensity dynamics. Above these bifurcations the dynamic behavior exhibited by the model is extremely rich. It has been found that the routes to chaos almost always involve quasiperiodic as well as intermittent dynamics. When this quasiperiodic behavior is locked, type-I and -II intermittencies have been identified. When unlocked, the torus can destabilize through two different scenarios leading to chaos: a ''quasiperiodic intermittency'' or a cascade of period-doubling bifurcations. On-off intermittency has also been found. [S1063-651X(97)04512-1]

PACS number(s): 05.45.+b, 42.65.Sf, 42.55.Ah

I. INTRODUCTION

In this paper we study numerically the temporal dynamics of a $J=0\leftrightarrow J=1$ Zeeman laser model. As will be shown in detail throughout the paper, the dynamics exhibited by the model involves both quasiperiodic and intermittent dynamics. The interest of our results resides in the peculiarity of the intermittencies that we find since, often, they are intimately related to quasiperiodic motions.

The intermittency scenario is one of the three possible ways along which a periodic behavior can continuously be transformed into a chaotic one, the other two being the quasiperiodic (or Ruelle-Takens) and period-doubling (or Feigenbaum) scenarios [1,2]. Intermittency is characterized by phases of almost periodic behavior interrupted by sudden chaotic bursts in such a way that the duration of the regular (or laminar) phases verify certain statistical regularities. In particular, the mean duration of the laminar phases shortens, following well-defined laws as chaos is approached. In their seminal paper [3], Pommeau and Manneville established the existence of up to three types of intermittency which differ in the way in which a periodic orbit loses its stability. The classification is made according to the way the eigenvalues of the differentiable Poincaré map cross the unit circle at the instability point: type I is associated with one real eigenvalue $(+1)$, and corresponds to a tangent bifurcation; type II is associated with a pair of complex-conjugate eigenvalues, and corresponds to something similar to a subcritical Hopf bifurcation; and type III is associated with a real eigenvalue (-1), and corresponds to a subcritical period-doubling bifurcation. In all three cases a reinjection mechanism is necessary in order to approach the trajectory to the unstable periodic orbit after every irregular burst (for details, see Refs. [1,2]).

Since the paper by Pommeau and Manneville, more types of intermittent behavior have been identified. In particular, type-*X* intermittency [4] was introduced in order to extend the type-I intermittency to cases in which the intermittency occurs near a hysteretic transition, and type *V* [5] was introduced for discontinuous maps; the crisis-induced intermittency [6] accounts for the long transients that appear when the coalescence between two unstable fixed points or periodic orbits and a strange attractor (with a fractal basin boundary) occurs, and in the on-off intermittency [7] the laminar phases correspond to the null value of a certain variable that switches on chaotically due to some external random variation of the parameters or to the chaotic motion of other system variables. Most of these types of intermittency have been predicted in physical models and observed experimentally. In particular, we found the on-off intermittency scenario in the Zeeman laser model that we study in the present paper [8], as we show below.

Of the three classical types of intermittency the most elusive one is type II. As far as we know there are very few theoretical predictions and experimental observations. The first theoretical prediction was made in Ref. [9] for a periodically driven nonlinear oscillator model. Recently some of us found this intermittency in a cascade laser model [10] that resembles in some aspects the laser model studied here. Also, in laser physics, type-II intermittency has been numerically observed in a model of a laser with saturable absorber with external excitation [11]. With respect to experimental observations, the first one was made by Huang and Kim in an electronic oscillator [12], an *inverted* type-II intermittent behavior was found by Sacher, Elsässer, and Göbel in a semiconductor laser [13], and there was a very clear observation in Ref. [14] during the oxidation of methanol.

In Ref. [10] we also found what seems to be a different type of intermittency that is similar in some aspects to the type-II intermittency, but that is associated to quasiperiodic motion. In it, the laminar phases are not periodic but quasiperiodic. We will find this new type of intermittent dynamics again in the Zeeman laser model analyzed here. Let us insist that this quasiperiodic intermittent behavior is a different type of intermittency, since the quasiperiodic nature of the laminar phases cannot be understood within the standard intermittency theory [1,2]. However, before entering into a description of the dynamic behaviors, we find it is necessary to comment on the physical model we study.

Dynamical properties of nonlinear optical systems, in which the polarization of the fields involved in the interaction plays a significant role, is a subject of present interest. This is because for a long time the light field has been treated as a scalar quantity in the dynamical studies of such systems, in spite of the fact that this assumption removes an important

degree of freedom. The reasons for this previous neglect of the vector character of the light are, on the one hand, the important simplification of the problem that this approximation implies and, on the other hand, that real systems include polarizing elements (such as Brewster windows in lasers) that fix the polarization field state.

Nevertheless, this is not always the case in laser physics, and there was early interest in the polarization properties of the light emitted by isotropic lasers (see Refs. [15–17], and references therein). This interest led to the identification of the conditions under which a laser based on a given $J \leftrightarrow J'$ transition would emit with linear or circular polarization [17]. Unfortunately these studies were made in the framework of the third-order Lamb theory, which is valid only for pump values close to the emission threshold. However, if one is interested in the nonlinear dynamical properties of a laser, one must take into account a more complete description that has no restrictions with respect to the pump values and to the matter relaxation constants values. At present the situation has drastically changed, and the number of papers in which the polarization of the fields is explicitly taken into account has increased during the last few years. In particular, there have been studies on two-level Zeeman lasers [8,18–25], optically pumped lasers [26–28], cascade lasers [29], fiber lasers [30,31] and vertical cavity surface-emitting lasers [32–34] including transverse phenomena [35,36].

As far as we know, the first study of the nonlinear dynamics of a laser model that did not put any restriction on the field polarization state was that of Puccioni *et al.* [18], in which the stability of a two-level Zeeman laser model based on a $J=1 \leftrightarrow J=0$ atomic transition was analyzed. In that work it was found that besides the usual Lorenz-Haken instability [37,38] (a subcritical Hopf bifurcation that destabilizes the laser intensity giving rise to chaotic dynamics and that appears for large values of both the cavity losses and pump parameters), there appears a second Hopf bifurcation that leads to a modification of the polarization state of the field. Moreover, this polarization instability usually occurs for pump and cavity loss parameter values much less restrictive than those imposed by the Lorenz-Haken instability.

The dynamics of this model was recently investigated in the isotropic case [19]. In that paper a numerical study of the model of Puccioni *et al.* [18] was made (assuming equal cavity losses for both fields) for cavity loss values corresponding to the good cavity case, i.e., to the domain where the Lorenz-Haken instability does not exist. Emphasis was put on the nontrivial dynamics that the system exhibits when the polarization instability is crossed, a fact related to some phase instability effects. In a companion paper [20] the slightly anisotropic case was also treated, paying special attention to the polarization switching phenomenon that appears when the atom-cavity detuning is varied across resonance. After Ref. [19], Schrama *et al.* [21] identified analytically the solutions with elliptical polarizations that appear after the polarization instability. In the present paper we continue the work of Refs. [20–22] by studying the dynamic behavior of the model of Ref. [18] in the bad cavity limit, with special emphasis on the case of a laser cavity with large anisotropy.

Recently Abraham, Arimondo, and San Miguel [22], following previous work by Lenstra [17], proposed a modification of the model of Ref. [18] in order to improve the description of the material relaxation phenomena that occur in a gas of $J=1 \leftrightarrow J=0$ two-level atoms. This improvement of the model is important, since the anisotropy of the material medium strongly depends on the material relaxation rates, and then the polarization state selection, as well as its stability, are determined by the relaxation rates. Nevertheless, in the present work we will consider the simplest model of Puccioni *et al.* [18] (which is a limit of the more general model of Ref. [22] for low gas pressures) because we will concentrate on the case of large cavity anisotropy, a parameter domain where we expect that the influence of the medium anisotropy will be small. Moreover, our main interest is on the routes to chaos (scenarios) exhibited by the model, a kind of behavior where we do not expect that small model variations will be important. In fact, we found that the type of scenarios exhibited by the model of Ref. [18] have large similarities to the ones that we found in a cascade laser model [29], thus implying a certain degree of robustness of the scenarios with respect to changes in the model parameters that do not modify the main structure of the equations. Like the $J=1 \leftrightarrow J=0$ two-level Zeeman laser model, the cascade laser model involves three atomic level connected by two allowed dipolar transitions, leading to a V-type level configuration in the first case and to a ladder-type level configuration in the second case [39]. Thus one can expect certain similarities in the dynamical properties of both systems, although the physics and the parameter values are different in both cases.

The rest of the paper is organized as follows. In Sec. II, the model is presented and its domain of applicability is discussed. In Sec. III, the stationary solutions and their stability are studied. In this section we pay special attention to the impossibility of determining the real polarization state of the laser with this model. In Sec. IV, the dynamics of the model beyond the instability threshold is numerically investigated. We concentrate on the bad cavity limit with a large cavity anisotropy, where we find rich intermittent and quasiperiodic dynamics. Finally, in Sec. V the main conclusions are stressed.

II. MODEL

As in Refs. [8,18], we consider a unidirectional ring cavity filled with a gas of two-level atoms with angular momenta $J=0$ and 1 for the lower and upper levels, respectively. The medium is assumed to be homogeneously broadened and incoherently pumped. Furthermore, we will assume that the cavity frequency coincides with the atomic transition frequency, and that the dephasing collisions between atoms are negligible (i.e., we consider the radiative limit). In this case, the model studied by Puccioni *et al.* [18] and the one proposed by Abraham, Arimondo, and San Miguel [22] coincide, because all the atomic relaxation rates take their minimum value (which is the common relaxation rate of the level populations). In this case the model equations read

$$\dot{e}_x = \sigma(p_x - e_x), \tag{1a}$$

$$\dot{e}_y = \sigma(p_y - \alpha e_y), \tag{1b}$$

$$\dot{p}_x = -p_x + e_x D_x + e_y q, \tag{1c}$$

$$\dot{p}_y = -p_y + e_y D_y + e_x q^*, \tag{1d}$$

$$\dot{D}_x = (r - D_x) - [2(e_x^* p_x + e_x p_x^*) + (e_y^* p_y + e_y p_y^*)], \tag{1e}$$

$$\dot{D}_y = (r - D_y) - [(e_x^* p_x + e_x p_x^*) + 2(e_y^* p_y + e_y p_y^*)], \tag{1f}$$

$$\dot{q} = -q - (e_x p_y^* + e_y^* p_x), \tag{1g}$$

Equations (1) have been written in the $|J=1, J_i=0\rangle$ ($i=x,y,z$) basis, with z the field propagation axis, which has been chosen as the quantization axis. This causes the upper sublevel $|J=1, J_z=0\rangle$ to be coherently uncoupled with the lower lasing level $|J=0\rangle$. e_x and e_y are the linear polarization (Cartesian) components of the electric field, p_i and D_i are proportional to the polarization and atomic inversion associated with the transition $|J=1, J_i=0\rangle \leftrightarrow |J=0\rangle$, and q is proportional to the coherence between the upper sublevels $|J=1, J_x=0\rangle$ and $|J=1, J_y=0\rangle$. The parameter r represents the incoherent pumping rate (assumed to be equal for all the upper level sublevels). σ and $\alpha\sigma$ represent the cavity losses along the x and y directions, respectively, thus representing α the cavity anisotropy. For definiteness we choose $\alpha \geqslant 1$, thus y labels the direction in which the cavity losses are larger. In Eqs. (1) all the frequencies have been normalized to the (common) material relaxation rate.

A fundamental property of Eqs. (1) is their invariance under the transformations

$$(e_x, p_x) \rightarrow (e_x, p_x)\exp(i\varphi_x),$$

$$(e_y, p_y) \rightarrow (e_y, p_y)\exp(i\varphi_y), \quad q \rightarrow q\ \exp[i(\varphi_y - \varphi_x)], \tag{2}$$

with φ_x and φ_y *arbitrary* constant phases. Since the polarization state of light depends on the relative phase between the x and y components of the field, it is obvious that Eqs. (1) do not fix the polarization state of the field (this also applies to the detuned laser case not considered here).

Since Eqs. (1) correspond to a perfectly tuned laser cavity, we assume that the solutions (either stationary or time dependent) are resonant, i.e., they do not exhibit a frequency shift with respect to the common value of the cavity and atomic transition frequencies (there is no pulling and/or pushing effect). Nonresonant solutions, i.e., frequency pulled solutions, may also exist. Nevertheless, due to the symmetry properties of Eqs. (1), if a solution with frequency ω exists, another solution with the same amplitude and frequency $-\omega$ will do. The coexistence of this type of symmetrically detuned solutions gives rise to pulsing solutions that appear at a Hopf bifurcation point. This situation has been previously found in a resonant cascade laser model [39]. This assumption is physically feasible and is compatible with Eqs. (1). Thus we write

$$e_x = E_x\ \exp(i\varphi_x), \quad e_y = E_y\ \exp(i\varphi_y), \tag{3a}$$

with E_x and E_y *real* amplitudes, and φ_x and φ_y *arbitrary* constant phases. This form leads to

$$p_x = P_x\ \exp(i\varphi_x), \quad p_y = P_y\ \exp(i\varphi_y),$$

$$q = Q\ \exp[i(\varphi_y - \varphi_x)], \tag{3b}$$

with P_x, P_y, and Q real amplitudes. In terms of the real amplitudes, Eqs. (1) read

$$\dot{E}_x = \sigma(P_x - E_x), \tag{4a}$$

$$\dot{E}_y = \sigma(P_y - \alpha E_y), \tag{4b}$$

$$\dot{P}_i = -P_i + E_i D_i + E_j Q, \tag{4c}$$

$$\dot{D}_i = (r - D_i) - 2(2E_i P_i + E_j P_j), \tag{4d}$$

$$\dot{Q} = -Q - (E_x P_y + E_y P_x), \tag{4e}$$

with $i,j = x,y$ and $j \neq i$. Let us remark that the values of the *arbitrary* constant phases φ_x and φ_y do not appear in Eqs. (4), a fact that, as commented upon above, has important physical consequences since it is the phase difference ($\varphi_y - \varphi_x$) that determines the polarization state of light. Thus it is the initial condition the one that fixes the phase difference and, since this difference does not change in time, the one that determines the actual polarization state of light.

Finally, let us remark that outside the radiative limit, one should consider different relaxation rates for the polarizations ($\gamma_\perp$), the population differences ($\gamma_\parallel$), the coherence Q (γ_c) as well as include a new variable (the difference of the upper sublevels populations) with a different relaxation rate (γ_J) [22]. When doing this the $|J=1, J_z=0\rangle$ upper sublevel appears involved in the dynamics through its incoherent coupling with the rest of levels. Thus Eqs. (4) are strictly valid only in the radiative limit. Nevertheless, as commented upon above, we can be confident that for large cavity anisotropies (i.e., large values of α) our predictions will remain accurate, since in this case the medium anisotropy can be neglected, at least in a certain range of low gas pressures.

III. STEADY SOLUTIONS AND THEIR STABILITY

Equations (4) have three sets of steady states, which are the off state

$$E_x = E_y = P_x = P_y = Q = 0, \quad D_x = D_y = r, \tag{5}$$

the linearly polarized state along the x direction,

$$E_x = P_x = \pm\frac{1}{2}\sqrt{r-1}, \tag{6a}$$

$$D_x = 1, \quad D_y = \frac{1}{2}(r+1), \tag{6b}$$

$$E_y = P_y = Q = 0, \tag{6c}$$

and a linearly polarized state along the y direction that for $\alpha = 1$ is given by Eq. (6) replacing x with y, but it is always unstable for $\alpha > 1$. Thus we will not consider this last solution in the following.

In the isotropic case $\alpha = 1$, Eqs. (4) also have the steady state (Refs. [8,18–22])

$$E_x^2+E_y^2=\tfrac{1}{4}(r-1), \quad P_x=E_x, \quad P_y=E_y, \tag{7a}$$

$$D_x=1+2E_y^2, \quad D_y=1+2E_x^2, \quad Q=-2E_xE_y, \tag{7b}$$

and represents the only case in which both field components are excited in a steady state (two-mode steady state).

Throughout this paper we will be mainly concerned with the anisotropic case ($\alpha>1$), and thus not much attention will be paid to the two-mode steady state since it does not exist for $\alpha>1$. Nevertheless it is worth insisting that, as opposed to the anisotropic case in which the polarization of solution (6) is perfectly defined, in the isotropic case there is a complete degeneracy of solutions all of them having the same intensity $I=E_x^2+E_y^2$. Thus solution (7) describes equally circularly polarized light [$E_x^2=E_y^2=I/2$, ($\varphi_y-\varphi_x=\pm\pi/2$)], linearly polarized light [$E_x^2=E_y^2=I/2$, ($\varphi_y-\varphi_x=0,\pi$)], or any other state of light.

Obviously the same difficulty is found when characterizing the polarization state in the dynamical regime (see below). Thus, although the nomenclature of linear and circular polarized solutions has been applied to the solutions of this model [18–22], it would be more appropriate to speak of one and two-mode solutions specifying the atomic basis in which the equations are written (a ''circular'' solution in our case is a two-mode solution but if the equations were written in the $\{J_z=+1, J_z=0, J_z=-1\}$ basis, it would be a one-mode solution). Of course this indetermination does not apply to the linearly polarized solution (6) when there is a cavity anisotropy (i.e., a preferred direction in the space) since in this case, this steady solution is the only existing one.

We now consider the stability of the steady states. The stability analysis of the off-state solution shows that it suffers a pitchfork bifurcation at the pump value $r=1$. Above this value the off state becomes unstable, and the lasing solution appears.

The stability of the lasing state is governed by a seventh-order characteristic equation that appears factorized into three polynomials:

$$(\lambda+1)AB=0, \tag{8a}$$

$$A=\lambda^3+(\sigma+2)\lambda^2+(\sigma+r)\lambda+2\sigma(r-1), \tag{8b}$$

$$B=\lambda^3+(\alpha\sigma+2)\lambda^2+\frac{1}{4}[3+r-2\sigma(1+r-4\alpha)]\lambda + \frac{1}{4}\sigma(r+3)(\alpha-1). \tag{8c}$$

Polynomials A and B give rise to a Hopf bifurcation each of them. These bifurcations occur at

$$r=r_{\mathrm{LH}}=\frac{\sigma(\sigma+4)}{\sigma-2} \tag{9a}$$

for cavity losses values larger than

$$\sigma_{\mathrm{BCL(LH)}}=2, \tag{9b}$$

which is the well-known Lorenz-Haken instability [37,38], and at

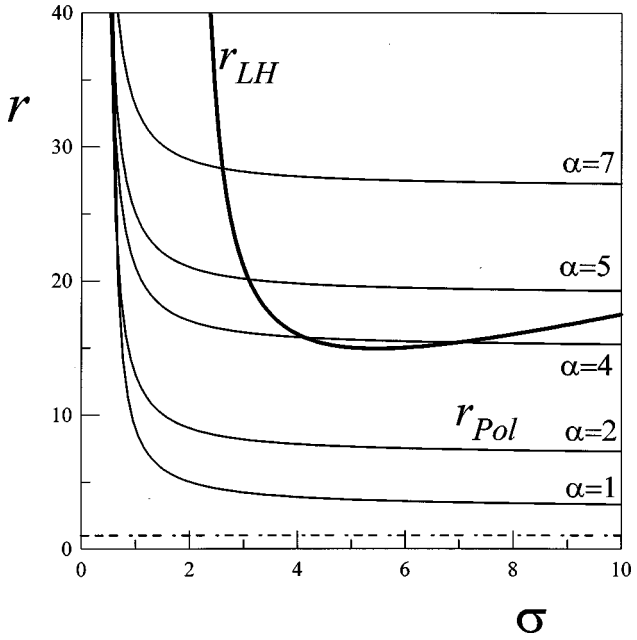

FIG. 1. Lorenz-Haken (thick line) and polarization instability thresholds for several values of the anisotropy parameter (α). The dashed line marks the lasing threshold.

$$r=r_{\mathrm{Pol}}=(2\alpha\sigma+1)\,\frac{6+\sigma(4\alpha-1)}{2\alpha\sigma^2+3\sigma-2}, \tag{10a}$$

for cavity losses values larger than

$$\sigma_{\mathrm{BCL(Pol)}}=\frac{-3+\sqrt{9+8\alpha}}{4\alpha}, \tag{10b}$$

which is the generalization of the polarization instability first described in the isotropic case ($\alpha=1$) by Puccioni *et al.* [18].

In the isotropic case, these instability boundaries are also valid and thus the two-mode steady states (7) are stable (marginally stable, in fact, due to the relative phase indetermination) for pump values below boundaries (9) or (10). This was not clearly appreciated in Refs. [18–22]. In fact the instability boundaries for $\alpha=1$ can be directly obtained from those of Ref. [22] by taking all the material relaxation rates equal to unity in them.

The linearly polarized solution given by Eqs. (6) becomes unstable for pump values larger than r_{LH} or r_{Pol}. In Fig. 1 the instability boundaries are represented in the $\langle r,\sigma\rangle$ plane for several values of the cavity anisotropy parameter α. The Lorenz-Haken instability curve remains unchanged since it is not affected by α, and it can be seen how larger values of the pump are necessary for reaching the polarization instability as α increases. When α tends to infinity, the model of Eqs. (4) reduces to the Lorenz-Haken model, since in this case a single (linear) polarization component of the field can be supported by the resonator, and a scalar treatment holds.

IV. DYNAMIC BEHAVIOR

In this section the dynamic behaviour of the system is analyzed. For doing that we will first present bifurcation diagrams in the $\langle\sigma,r\rangle$ plane corresponding to several values of

the cavity anisotropy parameter α. This will allow us to obtain a global perception of the dynamics of the system, which is clearly dominated by quasiperiodic and chaotic motions. Later we will analyze in detail several special scenarios in which type-I, type-II, and on-off intermittencies have been clearly identified. A different type of intermittency (''quasiperiodic'' intermittency) will be also presented, as well as a rich transition to chaos involving a period-doubling torus.

A. Bifurcation diagrams

In Figs. 2(a)–2(d) we show the bifurcation diagrams in the $\langle \sigma, r \rangle$ plane obtained for $\alpha = 1$, 2, 4, and 7, respectively. Although for the perfectly isotropic case ($\alpha = 1$) the adequacy of the model is not very large, as previously commented, we present its corresponding bifurcation diagram for the sake of completeness. Several conclusions can be extracted. In all the figures the stable steady state for small values of the pump r is the linearly polarized state ($E_x \neq 0$, $E_y = 0$), but for $\alpha = 1$ the polarization state is not determined, as we have stated. This linearly polarized state becomes unstable by increasing pump values when either the curves r_{Pol} or r_{LH} (the Hopf bifurcations of the system) are crossed.

In Fig. 2(a) ($\alpha = 1$), it can be seen that the leading bifurcation is the polarization one. When crossing it the dynamics is periodic, and involves oscillations in the two field components E_x and E_y. The periodic attractor appears smoothly from the steady state because the polarization bifurcation is supercritical. This periodic dynamics is destabilized to a quasiperiodic motion that occupies a narrow region in the parameter space, and that further destabilizes increasing the pump parameter r to a chaotic attractor. Thus, the scenario is the Ruelle-Takens-Newhouse one [40]. Let us stress that although both fields E_x and E_y oscillate after the polarization instability, nothing can be said with respect to the actual polarization state since the relative phase between the two fields is absolutely undetermined.

When cavity anisotropy is considered, the dynamics becomes much richer. In Fig. 2(b) the cavity anisotropy can be said to be moderate ($\alpha = 2$). As for $\alpha = 1$, the dominating bifurcation remains the polarization one, that again is supercritical. As a result, the truly linearly polarized steady state continues destabilizing to a periodic attractor. But now, as opposed to the previous case, there are several types of periodic attractors [we have found up to four of them, and their domains of stability are marked in Fig. 2(b)] that coexist in certain domains of the parameter space (not shown in the figure). When the pump value is increased these attractors become quasiperiodic, but this quasiperiodic motion is stable in a very small domain of parameters, and the trajectory in the phase space falls into the next periodic attractor. The last of these periodic attractors also becomes quasiperiodic. By further increasing r the quasiperiodic attractor becomes chaotic through an intermittent scenario.

For $\alpha = 4$ [Fig. 2(c)] the bifurcation diagram becomes much more involved. An important difference from the previous cases is that the two Hopf bifurcations (the Lorenz-Haken and polarization bifurcations) have approached each other considerably. Notice that for cavity losses smaller than $\sigma \approx 4$ and larger than $\sigma \approx 7$, the polarization bifurcation still dominates over the Lorenz-Haken one, which is subcritical.

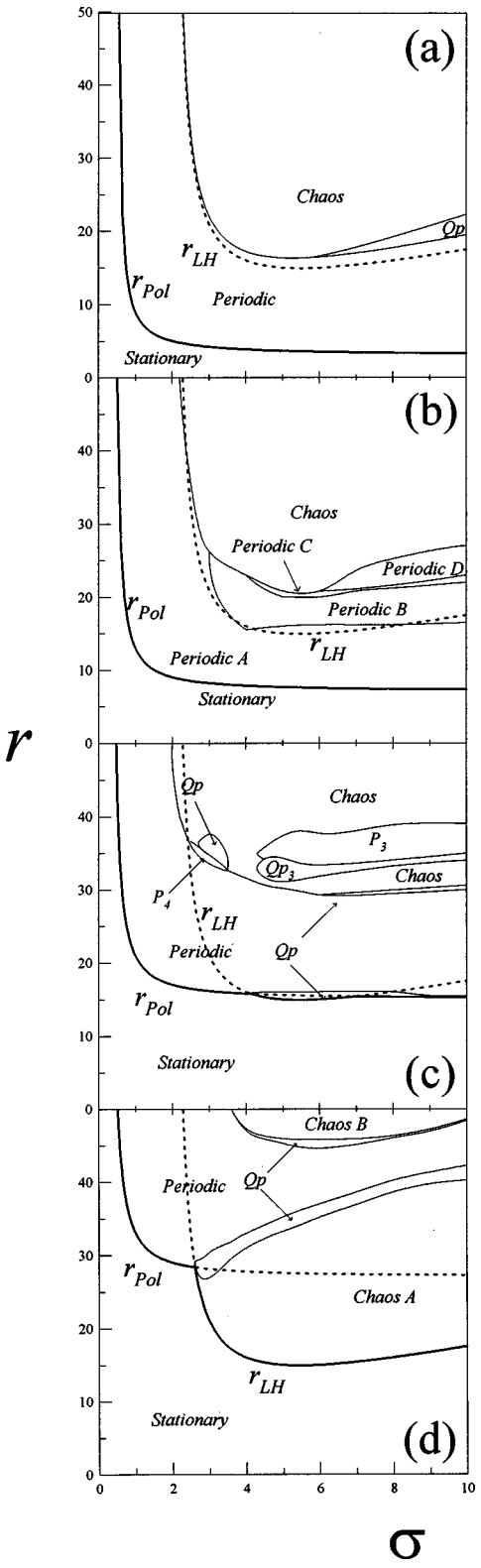

FIG. 2. Bifurcation diagrams for several values of the anisotropy parameter (α).

Thus for cavity losses in which the stability is governed by the polarization bifurcation the transition is from steady to periodic motion. But for cavity loss values where the two bifurcations are close (roughly $\sigma \in [4,8]$), there is a mutual influence between the two bifurcations that makes the destabilization of the steady state occur in a quasiperiodic motion.

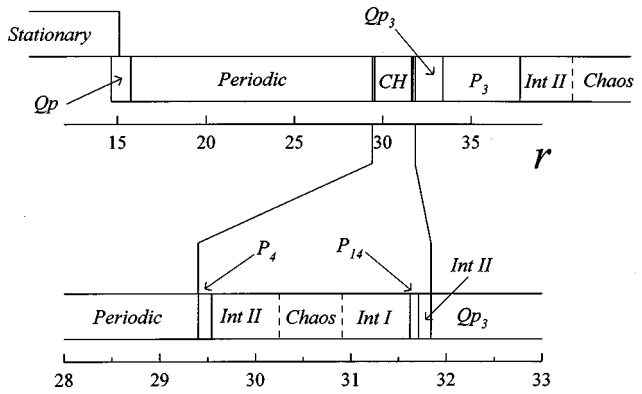

FIG. 3. Sequence of bifurcations for increasing pump values (r) for $\alpha=4$ and $\sigma=6$.

Nevertheless the domain where this quasiperiodic motion is stable is small, and periodic oscillations are recovered for pump parameter values slightly exceeding the bifurcation values. For increasing pump values there is a transition to chaos and, as for $\alpha=2$, this occurs through a mixture of the quasiperiodic and intermittent scenarios.

A concrete example of this type of bifurcation diagram is the one corresponding to $\alpha=4$, $\sigma=6$, and increasing pump values, shown in Fig. 3. First the linearly polarized steady state destabilizes to a torus due to the proximity of both Hopf bifurcations. By increasing r, the dynamics becomes periodic. The periodic attractor destabilizes to a period-4 periodic attractor P_4 (i.e., the field intensity pattern repeats after four peaks) which corresponds to a frequency locking of a quasiperiodic attractor (we know this because P_4 is continuous with a torus that exists for values of σ close to the one in the figure). From P_4 there is a transition to chaos via a type-II intermittency followed by an inverse type-I intermittency scenario (which is the one we analyze in Sec. IV C). This intermittency ends in a period-14 (P_{14}) periodic attractor. Further increasing the pump value P_{14} becomes a quasiperiodic attractor (QP_3 in the figure) through a complicated intermittent behavior that seems to be a type-II intermittency. This torus locks, leading to a period-3 periodic (P_3) attractor which finally destabilizes to chaos via type-II intermittency.

Let us finally consider the case of large cavity anisotropy $\alpha=7$ [Fig. 2(d)], which qualitatively represents what occurs for α values larger than, roughly, 4.5. In this case the stability of the linearly polarized steady state is dominated by the Lorenz-Haken instability for cavity loss values within the domain delimited by the two codimension-2 points defined by the crossings of the two bifurcations. As in the Lorenz-Haken model, crossing this bifurcation leads to Lorenz chaos. But this chaotic behaviour only affects to the subspace defined by $\{E_x,P_x,D_x,D_y\}$, and the rest of system variables (i.e., $\{E_y,P_y,Q\}$) remain in their steady (null) values. This is true for pump values not very far from the bifurcation value. When r is further increased, the null variables begin to oscillate chaotically at random instants of time, returning to the null value after each switching-on period. As the pump value is increased, the duration of the off states is shorter, until eventually all the variables behave chaotically. This is the on-off intermittency scenario [7], that we analyzed in detail in Ref. [8]. We will return to it, briefly, in Sec. IV F.

For larger pump values the chaotic dynamics is stabilized through an inverse quasiperiodic scenario. Within the quasiperiodic domain we have found very complex dynamics, such as a period-doubling torus that will be analyzed in Sec. IV B. Also, a quasiperiodic intermittency is present. For larger pump values the periodic behavior is again destabilized to a quasiperiodic attractor that leads to chaos via intermittency.

In order to clarify the rich phenomenology described above, we next summarize our observations. For values of α smaller than 4.5, the polarization instability is the first to be reached for all values of σ. In this case we find the basic sequence

$$\mathrm{SS}\rightarrow P\rightarrow \mathrm{QP}\rightarrow \mathrm{QP\ \ INT}\rightarrow \mathrm{CH},$$

where SS, P, QP, INT, and CH mean steady state, periodic attractor(s), quasiperiodic attractor, intermittency, and chaos, respectively. For α larger than 4.5, the first bifurcation is the Lorenz-Haken one for large enough cavity losses. In this case the basic sequence is

$$\mathrm{SS}\rightarrow \mathrm{Lorenz\ \ CH}\rightarrow \mathrm{on\text{-}off\ \ INT}\rightarrow \mathrm{CH}\rightarrow \mathrm{QP\ \ INT}\rightarrow \mathrm{QP}\rightarrow P$$
$$\rightarrow \mathrm{QP}\rightarrow \mathrm{type\ \ II\ \ INT}\rightarrow \mathrm{CH}.$$

Thus, the transitions from periodic behavior to chaos are dominated by quasiperiodic attractors independently of the α value. But as α increases it becomes more clear that the actual scenarios are the intermittent ones. When the quasiperiodic attractors are frequency locked it is more or less easy to identify type-I and -II intermittencies (we have never seen type III), but, when the torus is unlocked, the type of intermittency is obviously different, and cannot be assimilated to any of the known intermittencies. Another clear conclusion is that, for large α values, the transition to fully developed chaos in the model occurs directly from the steady state via the on-off intermittency, whenever the Lorenz-Haken bifurcation dominates the stability of the steady state. In the following subsections we show examples, with their corresponding characterizations, of each of the encountered scenarios.

B. Period-doubling torus

A remarkable result of our study corresponds to the complicated transformations that a torus can develop during its transition to chaos [41–44]. Figure 4 shows the first return map for the cascade of different quasiperiodic behaviors observed for $\alpha=7$ and $\sigma=6$. For decreasing pump value, the initial T^2 torus in Fig. 4(a) suffers two consecutive period doubling bifurcations, Figs. 4(b) and 4(c). [The corresponding frequency spectra are shown in Figs. 5(b)–5(d), see caption]. For still lower r the torus becomes a strange attractor that seems to be a T^3 torus [Fig. 4(d)], as was also found in Ref. [41]. However, it has been impossible to find this third frequency by studying its power spectrum [Fig. 5(e)]. The final transition to chaos occurs through a intermittent behavior that will be analyzed in Sec. IV E.

Such a cascade of dynamical behaviors varies drastically as σ is changed. This is due to two different processes that can alter the steps of the cascade. On the one hand we see that the tori may suffer destabilizations that lead directly to

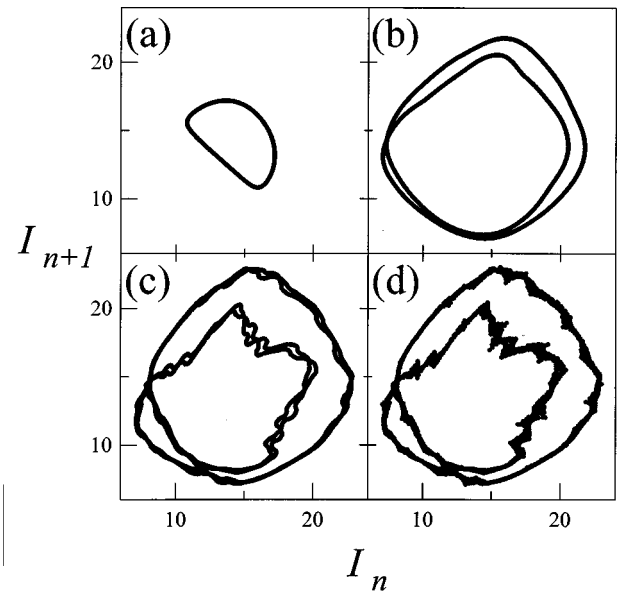

FIG. 4. First return maps for $\alpha=7$, $\sigma=6$, and $r=36.6$ (a), $r=35.9$ (b), $r=35.145$, (c), or $r=35.141$ (d).

chaos. This is because, as r is changed, the tori become more fragile and unstable, and in that case the destabilizations interrupts the cascade. On the other hand, frequency lockings (which are quite common in our model) change the steps of the cascade in different ways depending on the stage at which the frequency locking occurs. In particular, frequency locking transforms the quasiperiodic intermittency (Sec. IV E) in type-II intermittency (Sec. IV D).

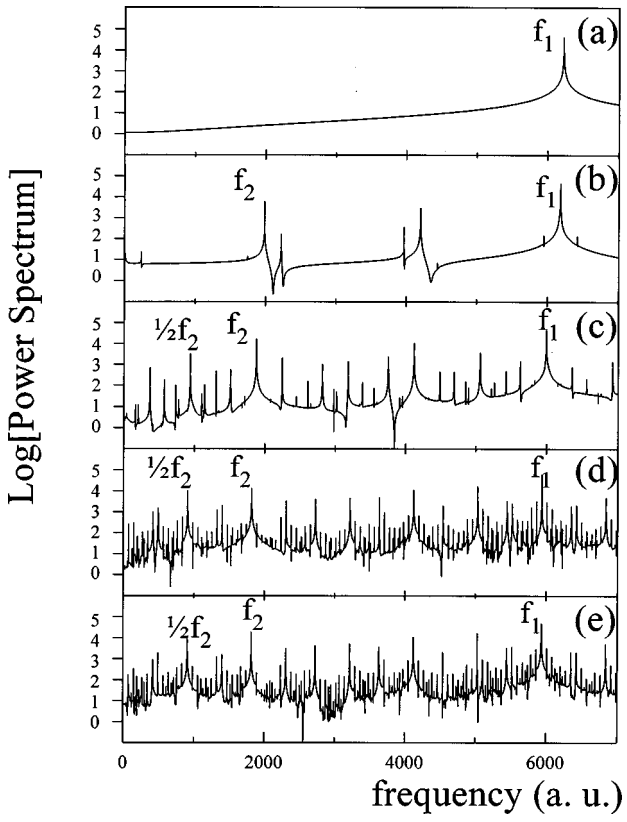

FIG. 5. Power spectrum for $\alpha=7$, $\sigma=6$, and $r=37$ (a), $r=36.6$ (b), $r=35.9$ (c), $r=35.145$ (d), or $r=35.141$ (e).

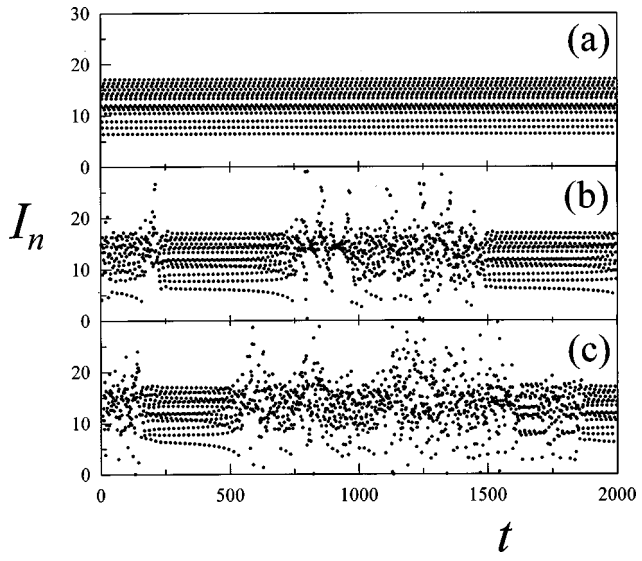

FIG. 6. Intensity maxima series for $\alpha=4$, $\sigma=6$, and $r=31.62$ (a), $r=31.61$ (b), or $r=31.60$ (c).

C. Type-I intermittency

We have seen only one case in which the transition from a locked torus to chaos occurs via type-I intermittency. It corresponds to the transition from chaos to P_{14} in the case $\alpha=4$ and $\sigma=6$ shown in Fig. 3, commented upon above.

Figure 6 shows the time evolution of the intensity maxima of the x component of the field (E_x^2) for three decreasing values of the pump parameter r (see caption) The intensity maxima evolution is shown for the sake of clarity, since in the whole intensity evolution it is impossible to identify any clear feature. Although the laminar phases look quite complex, the existence of 14 structures can be recognized. The first return map of one of these structures is shown in Fig. 7(a), and the parabolic shape of the map, characteristic of this type of intermittency [1], is clearly apparent. In fact, this map can be converted into the form

$$x_{n+1}=\varepsilon+x_n+x_n^2, \tag{11}$$

which defines type-I intermittency. In Eq. (11) x_n is proportional to the intensity maxima I_n after a suitable rescaling and shifting have been used, and ε is the coupling parameter ($\varepsilon=0$ at the onset of intermittency).

We have constructed the probability distribution of the laminar phase duration, an example of which is shown in Fig. 7(b), and corresponds to the study of 10^5 laminar phases. It clearly exhibits two maxima, one for short and one for long laminar phases, as predicted by the type-I intermittency theory [1].

In order to characterize the intermittency better, we studied the dependence of the mean duration of a laminar phase, $\langle l\rangle$, with the pump parameter (r). Our results show the typical regularity of the intermittent phenomenon [1]. In particular we obtain a scaling law of the type $\langle l\rangle\propto(r-r_0)^{-\xi}$, with r_0 the pump parameter value at the intermittency onset. According to the standard theory of intermittency the expected law is $\langle l\rangle\propto\varepsilon^{-\beta}$, with $\beta=\frac{1}{2}$, with ε the control parameter appearing in Eq. (11), and $b=\frac{1}{2}\langle l\rangle\propto\varepsilon^{-\beta}$, with $\beta=\frac{1}{2}$ (although, recently, scaling laws with $\beta\neq 1/2$ and even of loga-

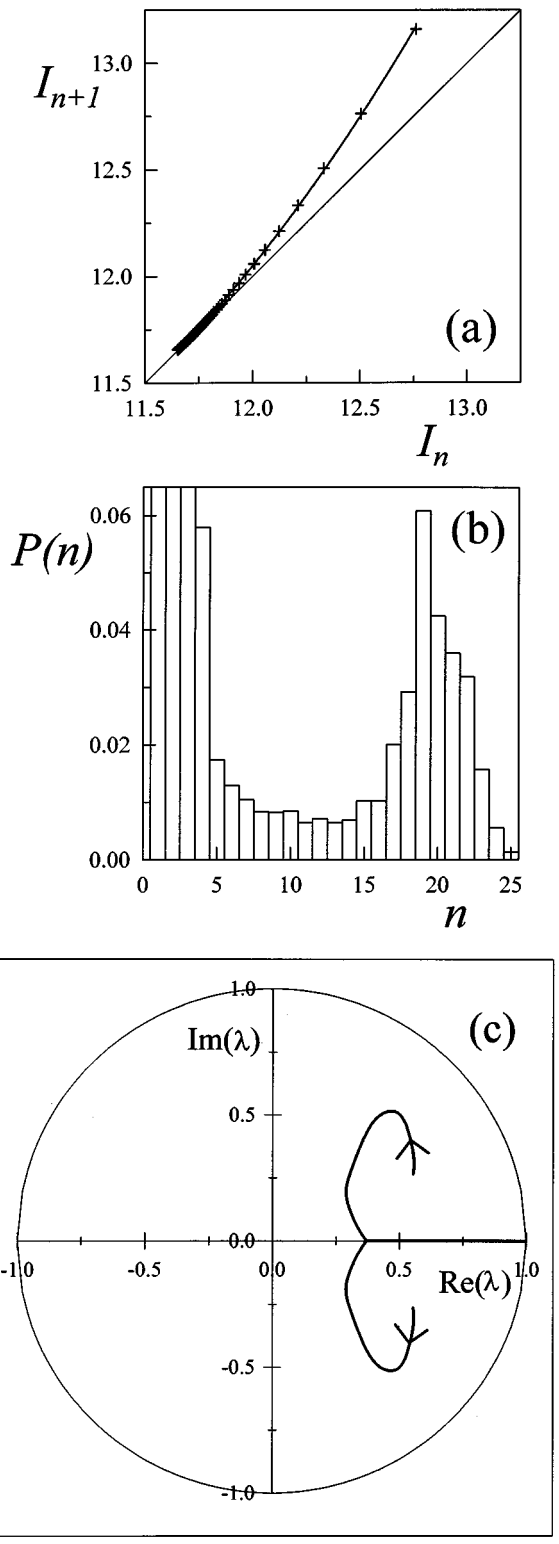

FIG. 7. First return map (a) and laminar phase duration histogram (b) for $\alpha=4$, $\sigma=6$, and $r=31.615$. In (c), the variation of the larger Floquet multipliers with r is shown for the same case.

rithmic form have been determined [45]). For checking this scaling law, it is necessary to determine the relation between the actual control parameter (the pump parameter r in our case) and ε. This can be done by using map (11) to determine the value of ε numerically, and then its relation with r by repeating the operation for several values of r. Indeed

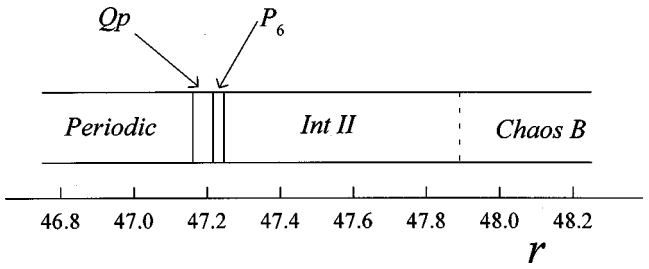

FIG. 8. Sequence of bifurcations for increasing pump values (r) for $\alpha=7$ and $\sigma=4$.

some of us used this method in Ref. [10]. Unfortunately, in the present case this is not very useful, because there is a great dispersion in the values obtained for ε. The same type of difficulty appears with the type-II intermittency analyzed in Sec. IV D.

Finally, there is another way of ensuring that the type of intermittency we are analyzing is type I. This can be done by calculating the evolution of the Floquet multipliers [1] of the periodic attractor (the P_{14} attractor in the present case) as the intermittency is approached. Figure 7(c) shows this evolution, and it is clearly seen that, although the larger Floquet multipliers are initially two complex-conjugate ones, they become real as the intermittency onset is approached in such a way that only one of them crosses the unit circle through $\lambda=1$ (the other Floquet multiplier moves leftwards on the real axis before reaching $\lambda=1$), as it corresponds to the type-I intermittency [1].

D. Type-II intermittency

Type-II intermittency is ubiquitous in the transitions to chaos in our system. We have chosen this particular case ($\alpha=7$, $\sigma=4$) for illustrating this scenario because it represents well what is observed for other parameter sets. The scenario is shown in Fig. 8 [compare with Fig. 4(d)]: the periodic attractor destabilizes to a quasiperiodic attractor which frequency locks, giving rise to a period-6, P_6, periodic attractor. After this P_6 attractor a type-II intermittency scenario follows, eventually leading to chaos.

The type-II intermittency is characterized by a two-dimensional map of the form [1]

$$\rho_{n+1}=(1+\varepsilon)\rho_n+\rho_n^3,$$
$$\theta_{n+1}=\theta_n+\phi, \tag{12}$$

where $\rho\exp(i\theta)$ is a complex variable and ε is the coupling parameter. Intermittency onset occurs at $\varepsilon=0$, and ϕ is a constant phase.

Figure 9 shows the intensity maxima time evolution for three increasing values of the pump r. A progressive shortening of the laminar phases is clearly noticeable. It can be appreciated that there are six different structures in the laminar phases, each of them showing a typical oscillation of type-II intermittency. Nevertheless, and contrary to the standard behavior [1], the frequency of this oscillation (related to ϕ) is not constant. Interestingly enough, this oscillation frequency even changes its sign. This is clearly appreciated as a change in the direction of the spiraling out in the first return

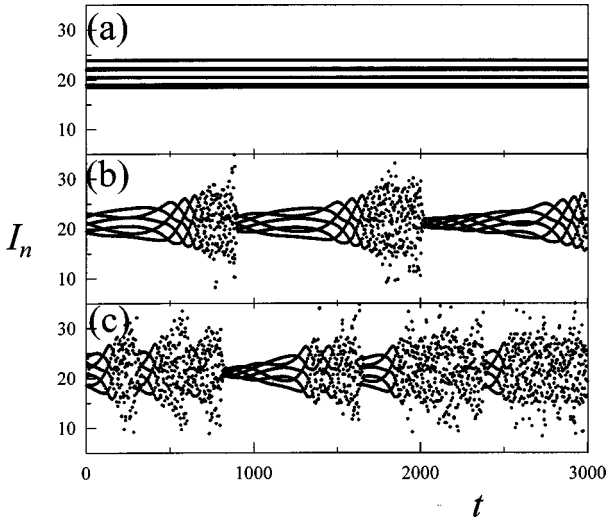

FIG. 9. Intensity maxima series for $\alpha=7$ and $\sigma=4$: $r=47.23$ (a), $r=47.30$ (b), and $r=47.40$ (c).

map, as can be seen in Fig. 10(a). These features are related with higher-order nonlinearities not considered in map (12).

In order to characterize this intermittent behavior better, we studied the distribution of the laminar phase duration, and the histogram is shown in Fig. 10(b). A single peak for short durations is observed, in agreement with theory [1]. Nevertheless this is not a sufficient signature of type-II intermittency, since for type-III intermittency the same behavior is predicted. Moreover, as for the case of the type-I intermittency analyzed in Sec. IV C, we do not have the possibility of determining the actual value of ε. Thus, as for type-I intermittency, we calculated the evolution of the Floquet multipliers of the periodic orbit as the pump parameter approaches the transition from periodic to intermittent behavior. A clearest signature of type-II intermittency is shown in Fig. 10(c): two complex-conjugate Floquet multipliers cross the unit circle with non-null imaginary parts.

Let us insist that type-II intermittency is commonplace in the Zeeman laser model we are considering, and remark that it appears in an unusual way: it is not a periodic attractor, but a frequency-locked quasiperiodic attractor, that destabilizes (this type of behavior was found previously by some of us in a cascade laser model [10]). This fact makes the number of nearly periodic structures that can be found in a laminar phase depend on the locking ratio. Moreover, in our example we showed the nonconstant character of the oscillation frequency along the laminar phases, a feature that cannot be reproduced with a standard type-II intermittency map [1].

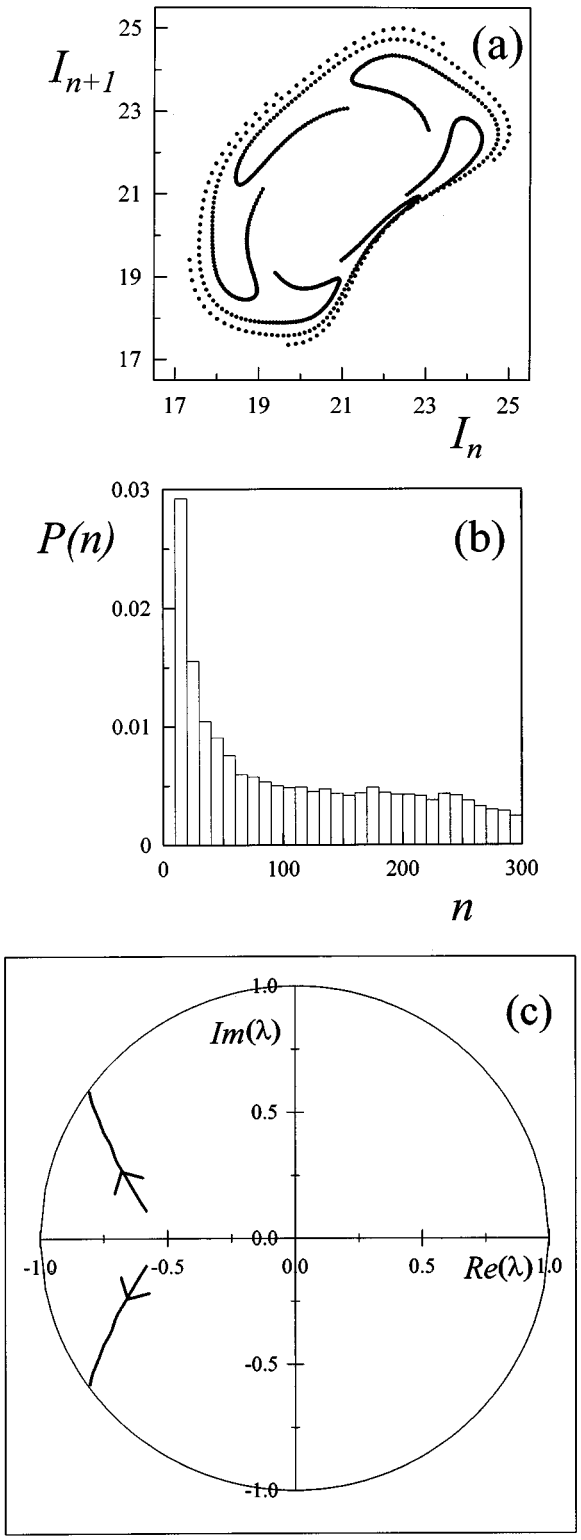

FIG. 10. First return map (a) and laminar phase duration histogram (b) for $\alpha=7$, $\sigma=4$, and $r=47.25$. In (c), the variation of the larger Floquet multipliers with r is shown for the same case.

E. Quasiperiodic intermittency

Although the type-I and -II intermittency behaviors analyzed above have some unusual features, the most exotic intermittency we found is what we call ''quasiperiodic'' intermittency. This kind of intermittent behavior was previously found in a cascade laser model [10], which shares some features with the model studied here. In this kind of behavior, a torus is destabilized, giving rise to an intermittency between laminar phases (in this case they are of quasiperiodic nature) and chaotic bursts, whose relative abundance is larger as the control parameter is moved away from the bifurcation point.

In Fig. 11 we show the intensity maxima evolution for three values of the pump parameter. Figures 11(a)–11(c) correspond to a T^3 torus, and intermittency with long and short

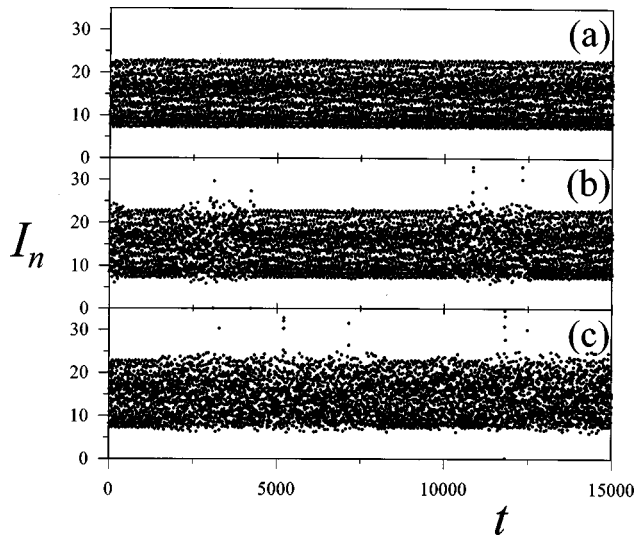

FIG. 11. Intensity maxima series for $\alpha=7$, $\sigma=6$, and $r=35.141$ (a), $r=35.1395$ (b), or $r=35.125$ (c).

laminar phases, respectively. In this case the structure of the laminar phases is much more complicated than in the case of Fig. 9, a fact that is better seen in the first return maps of Fig. 12 that correspond to the T^3 torus (a) (notice the broadening of the first return map typical of three-frequency quasiperiodicity), and to a single laminar phase (the denser part of the figure) including the beginning of the final burst (b).

We have not been able to make a clear statistical characterization of the laminar phase duration. The problem comes

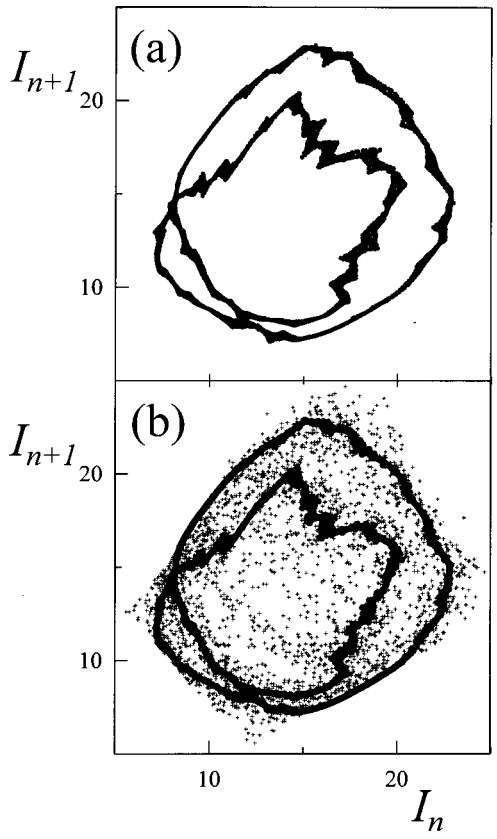

FIG. 12. First return maps for $\alpha=7$, $\sigma=6$, and $r=35.141$ (a), or $r=35.1395$ (b).

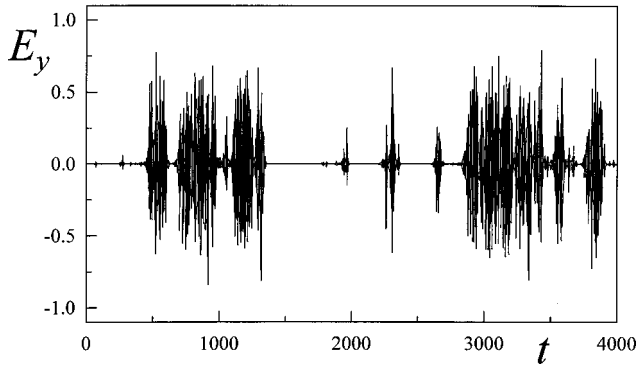

FIG. 13. Time series of the y component of the field for $\alpha=7$, $\sigma=4$, and $r=20.5$.

from the fact that it is usually very difficult to distinguish, in an automatic way, what is a laminar phase and what is not. Even in the cases in which the chaotic bursts are clearly separable from the laminar phases, we have been able to obtain only qualitative information: we see that the histogram of the laminar phase duration shows a single maximum for short laminar phases. This is, in principle, compatible with both type-II and -III intermittencies.

In any case we can affirm that this quasiperiodic intermittency does not correspond to any of the ones described in Ref. [3], because the first return map is absolutely different in this case. The only way of identifying and completely characterizing this new type of intermittency would be by constructing a map that could reproduce the quasiperiodic nature of the laminar phases.

F. On-off intermittency

There is still another type of intermittency present in the Zeeman laser model: the on-off intermittency. Since it was studied in detail in Ref. [8], we simply comment briefly on it for the sake of completeness.

As stated in Sec. IV A, whenever the bifurcation first crossed by the steady state is the Lorenz-Haken one, the variables $\mathbf{X}=\{E_x,P_x,D_x,D_y\}$ begin to oscillate chaotically, exhibiting Lorenz chaos, but the rest of variables $\mathbf{Y}=\{E_y,P_y,Q\}$ remain on its stationary value (which is the off state). This occurs because the hyperplane $\mathbf{Y}=0$ is invariant under the time evolution of $\mathbf{X}$, a fact that can be easily seen in Eqs. (4). Nevertheless, if the variables of $\mathbf{X}$ reach adequate values under time evolution, $\mathbf{Y}=0$ can be destabilized, and the variables $\mathbf{Y}$ can switch on during the time that the perturbation remains in its adequate value. This is on-off intermittency [7]. As the pump is increased, the switch-off periods are shorter, and eventually all the system variables behave chaotically. Figure 13 shows an example of the time evolution exhibited by the component E_y of the field in which the off-state laminar phases are clearly noticeable.

In Ref. [8] we studied the dependence of the laminar phase mean duration as a function of the pump parameter value, and confirmed the predictions of the on-off intermittency theory [46]: the probability of finding a laminar phase of length l is $l^{-3/2}$ for small l, and follows an exponential decay for large l, and the mean duration of the laminar phases depend on the coupling parameter as ε^{-1} near the intermittency onset. We also discussed the importance of the

way in which the laminar phases are counted in order to obtain the right exponent in this last law.

V. CONCLUSIONS

In this paper the dynamic behavior of the model of Puccioni *et al.* for a $J=0\leftrightarrow J=1$ Zeeman laser [18] generalized to anisotropic cavities has been analyzed, paying special attention to the case of large cavity anisotropy. We have discussed in detail the inability of the model to predict the polarization state of the light in the dynamic regime. In the isotropic case this indetermination extends even to the steady states of the system, as it also occurs in the more accurate model of Ref. [22].

We have analyzed the stability of the stationary solutions, showing how the competition between the two independent Hopf bifurcations present in the system (the Lorenz-Haken and the polarization instabilities) changes as a function of the cavity anisotropy parameter α. We have also analyzed how the dynamic behavior exhibited by the system depends on this factor.

In particular, we have shown that transitions to chaos may occur in three different ways: through the Ruelle-Takens-Newhouse scenario (for small values of α), through on-off intermittency (for values of α and σ, such that the first crossed bifurcation is the Lorenz-Haken one), and through a variety of intermittencies that are intimately related to quasiperiodic motions. These latter ones include both type-I and -II intermittencies (that occur when the quasiperiodic attractor is frequency locked), and a new type of intermittency (previously found by some of us [10] in a cascade laser model [39]) in which the laminar phases are quasiperiodic, and that we have named quasiperiodic intermittency.

This quasiperiodic intermittency occurs when the attractor is a T^3 unlocked torus. We have seen that in the this type of intermittency the laminar length distribution is such that short laminar phases are more probable (as it occurs with type-II and -III intermittencies), but we have not been able to characterize the statistics of these new intermittencies because of the difficulty in the automatic recognition of laminar phases.

Another instability mechanism affecting tori, consisting of a period-doubling cascade, has also been found. This mechanism has been found to be extremely sensitive to small parameter value variations. In particular, it is observed that the cascade sequence can change because of the appearance of frequency lockings, and because the stability of the intermediate period-doubled tori is not very robust.

With regard to the observability of these dynamical features, some comments are in order. The model studied here is strictly valid in the radiative limit, which implies low gas pressures. At the same time the scenarios described throughout this paper require large values of both the cavity losses and the pump. It seems difficult to find a laser that fulfills these conditions.

Nevertheless, as stated, we can expect the same type of scenarios to be found in the more complete model of Ref. [22], that is adequate for higher pressures since the modification of the relaxation rates does not modify the nonlinearities in the model, which determines the nonlinear dynamics. On the other hand, large values of the pump and the cavity losses can be simultaneously achieved for certain types of lasers (e.g., far-infrared ammonia lasers [47]). Moreover, the consideration of important physiocal factors such as Doppler broadening can considerably lower the thresholds without affecting seriously the type of dynamic behavior [48]. In conclusion, we can expect the type of dynamics described here to be observable in Zeeman lasers.

ACKNOWLEDGMENT

This work was supported by the DGICYT (Spain), Project No. PB95-0778-C02-01.

[1] H. G. Schuster, *Deterministic Chaos. An Introduction* (VCH, Weinheim, 1989).
[2] P. Bergé, Y. Pomeau, and Ch. Vidal, *Order within Chaos* (Wiley/Hermann, New York, 1986).
[3] Y. Pommeau and P. Maneville, Commun. Math. Phys. **74**, 189 (1980).
[4] T. J. Price and T. Mullin, Physica D **48**, 29 (1991).
[5] M. Bauer, S. Habip, D. R. He, and W. Matienssen, Phys. Rev. Lett. **68**, 1625 (1992).
[6] C. Gregobi, E. Ott, and J. A. Yorke, Phys. Rev. Lett. **50**, 935 (1983).
[7] N. Platt, E. A. Spiegel, and C. Tresser, Phys. Rev. Lett. **70**, 279 (1993).
[8] J. Redondo, E. Roldán, and G. J. de Valcárcel, Phys. Lett. A **210**, 301 (1996).
[9] P. Richetti, F. Argoul, and A. Arneodo, Phys. Rev. A **34**, 726 (1986).
[10] G. J. de Valcárcel, E. Roldán, V. Espinosa, and R. Vilaseca, Phys. Lett. A **206**, 359 (1995); **209**, 388(E) (1995).
[11] J. San Martín and J. C. Antoranz, Prog. Theor. Phys. **94**, 535 (1995).
[12] J.-Y. Huang and J.-J. Kim, Phys. Rev. A **36**, 1495 (1987).
[13] J. Sacher, W. Elsässer, and E. Göbel, Phys. Rev. Lett. **63**, 2224 (1989).
[14] H. Herzel, P. Plath, and P. Senesson, Physica D **48**, 340 (1991).
[15] H. de Lang, Philips Res. Rep. **8**, 1 (1967).
[16] W. Van Haeringen, Phys. Rev. **158**, 256 (1967).
[17] D. Lenstra, Phys. Rep. **59**, 299 (1980).
[18] G. Puccioni, M. V. Tratnik, J. E. Sipe, and G. L. Oppo, Opt. Lett. **12**, 242 (1987).
[19] N. B. Abraham, M. D. Matlin, and R. S. Gioggia, Phys. Rev. A **53**, 3514 (1996).
[20] M. D. Matlin, R. S. Gioggia, N. B. Abraham, P. Glorieux, and T. Crawford, Opt. Commun. **120**, 204 (1995).
[21] C. A. Schrama, M. A. van Eijkelenborg, L. P. Woerdman, and M. San Miguel, Opt. Commun. **138**, 305 (1997).
[22] N. B. Abraham, E. Arimondo, and M. San Miguel, Opt. Com-

mun. **117**, 344 (1995); **121**, 168(E) (1995).
[23] A. P. Voitovich, A. M. Kul'minskii, and V. N. Severikov, Opt. Commun. **126**, 152 (1996).
[24] L. P. Svirina, Opt. Commun. **111**, 370 (1994).
[25] R. J. Ballagh and N. J. Mulgan, Phys. Rev. A **52**, 4945 (1995).
[26] R. Corbalán, R. Vilaseca, M. Arjona, J. Pujol, E. Roldán, and G. J. de Valcárcel, Phys. Rev. A **48**, 1483 (1993).
[27] E. Roldán, G. J. de Valcárcel, R. Vilaseca, and R. Corbalán, Phys. Rev. A **49**, 1487 (1994).
[28] A. Kul'minskii, R. Vilaseca, and R. Corbalán, Opt. Lett. **20**, 2390 (1995).
[29] V. Espinosa, G. J. de Valcárcel, E. Roldán, and R. Vilaseca, J. Mod. Opt. **42**, 895 (1995).
[30] R. Leners and G. Stéphan, Quantum Semiclassic. Opt. **7**, 757 (1995).
[31] H. Zeghlache, Phys. Rev. A **52**, 4229 (1995); **52**, 4243 (1995).
[32] C. Serrat, N. B. Abraham, M. San Miguel, R. Vilaseca, and J. Martín-Regalado, Phys. Rev. A **53**, R3731 (1996).
[33] M. Travagnin, M. P. van Exter, A. K. Jansen van Doorn, and J. P. Woerdman, Phys. Rev. A **54**, 1647 (1996).
[34] J. Martín-Regalado, M. San Miguel, N. B. Abraham, and F. Prati, Opt. Lett. **21**, 351 (1996).
[35] M. San Miguel, Q. Feng, and J. V. Moloney, Phys. Rev. A **52**, 1728 (1995).
[36] M. San Miguel, Phys. Rev. Lett. **75**, 425 (1995).
[37] E. N. Lorenz, J. Atmos. Sci. **20**, 130 (1963).
[38] H. Haken, Phys. Lett. A **53**, 77 (1975).
[39] G. J. de Valcárcel, E. Roldán, and R. Vilaseca, Phys. Rev. A **45**, R2674 (1992); **49**, 1243 (1994).
[40] D. Ruelle, F. Takens, and D. Newhouse, Commun. Math. Phys. **64**, 35 (1978).
[41] V. Franceschini, Physica D **6**, 285 (1983).
[42] A. Arnéodo, P. H. Coullet, and E. A. Spiegel, Phys. Lett. **94A**, 1 (1983).
[43] O. Hess, D. Merbach, H.-P. Herzel, and E. Schöll, Phys. Lett. A **194**, 289 (1994).
[44] K. Kaneko, Prog. Theor. Phys. **69**, 1806 (1983).
[45] C.-M Kim, O. J. Kwon, E.-K. Lee, and H. Lee, Phys. Rev. Lett. **73**, 525 (1994).
[46] J. F. Heagy, N. Platt, and S. M. Hagel, Phys. Rev. E **49**, 1140 (1994).
[47] C. O. Weiss, R. Vilaseca, N. B. Abraham, R. Corbalán, E. Roldán, G. J. de Valcárcel, J. Pujol, U. Hübner, and D. Y. Tang, Appl. Phys. B: Photophys. Laser Chem. **61**, 223 (1995).
[48] E. Roldán, G. J. de Valcárcel, R. Vilaseca, R. Corbalán, V. J. Martínez, and R. Gilmore, Quantum Semiclassic. Opt. **9**, R1 (1997).